Journal of Neuroscience Methods 294 (2018) 40–50

Contents lists available at ScienceDirect

Journal of Neuroscience Methods

journal homepage: www.elsevier.com/locate/jneumeth

Research Paper

A new rat-compatible robotic framework for spatial navigation behavioral experiments

Sam Gianelli[a], Bruce Harland[a,b], Jean-Marc Fellous[b,c,*]

[a] Computational and Experimental Neuroscience Laboratory, University of Arizona, United States
[b] Psychology Department, University of Arizona, United States
[c] Program in Applied Mathematics University of Arizona, Tucson, AZ, United States

HIGHLIGHTS

- Novel robotic framework for rodent spatial navigation experiments.
- Precise control of animal direction and speed.
- Robot-assisted maze teaching.
- Compatible with electrophysiological recordings.
- Usable in large and complex spatial environments.

ARTICLE INFO

Article history:
Received 7 June 2017
Received in revised form 23 October 2017
Accepted 23 October 2017
Available online 4 November 2017

Keywords:
Robot
Sphero
Spatial navigation
Place-cell
Hippocampus

ABSTRACT

Background: Understanding the neural substrate of information encoding and processing requires a precise control of the animal's behavior. Most of what has been learned from the rodent navigational system results from relatively simple tasks in which the movements of the animal is controlled by corridors or walkways, passive movements, treadmills or virtual reality environments. While a lot has been and continues to be learned from these types of experiments, recent evidence has shown that such artificial constraints may have significant consequences on the functioning of the neural circuits of spatial navigation.
New methods: We present a novel and alternative approach for effectively controlling the precise direction and speed of movement of the animal in an ethologically realistic environment, using a small robot (Sphero).
Results: We describe the robotic framework and demonstrate its use in replicating pre-programmed or rat-recorded paths. We show that the robot can control the movement of a rat in order to produce specific trajectories and speeds. We demonstrate that the robot can be used to aid the rat in learning a spatial memory task in a large and complex environment. We show that dorsal hippocampal CA1 place cells do not remap when the rat is following the robot.
Comparison with existing method(s): Our framework only involves positive motivation and has been tested together with wireless electrophysiology in large and complex environments.
Conclusions: Our robotic framework can be used to design novel tasks and experiments in which electrophysiological recordings would be largely devoid of maze or task-dependent artifacts.

1. Introduction

The reproducibility of behavior across different animals and multiple sessions is key to the ability to aggregate data and to discover behavioral or neurophysiological features leading to scientific insights.

In the case of rodent spatial navigation, the direction of movement and the speed of the animal are notoriously difficult to control. Popular methods to control direction of movement include having the rat traverse a maze-like environment where the rat's trajectory is in large part determined by arrangements of tall, narrow corridors such as in the study of head direction information using a "hairpin maze" (Derdikman et al., 2009; Whitlock and Derdikman, 2012). In such mazes, the animal trajectory is constrained to specific

* Corresponding author at: University of Arizona, 1503 E University Blvd, Room 312, Tucson AZ, 85721, United States.
E-mail address: fellous@email.arizona.edu (J.-M. Fellous).

https://doi.org/10.1016/j.jneumeth.2017.10.021
0165-0270/

directions, with the side effect of fragmenting space into sub-spatial domains, possibly engaging ethologically unrealistic navigation mechanisms. Others use elevated walkways to limit the animal's spatial decisions to only a few, usually highly symmetric and easy to analyze paths, such as with the radial maze apparatus or linear track. Significant differences have been seen between wall-rich environments and unrestricted open fields, resulting from a temporally dynamic mixture of navigational stereotypy and use of local cues (Navratilova et al., 2012).

Speed is almost impossible to control naturally, as rats cannot be conditioned to walk or run at specific speeds. Early work involved restraining the animal and moving it by hand (Foster et al., 1989), or on an electric car or train (Terrazas et al., 2005). Both methods showed the importance of self-motion for well-formed hippocampal place-cell firing (Foster et al., 1989). To keep self-motion information unaffected, others have opted for limiting the animal movements to a computer controlled treadmill (or ball) apparatus (Fox et al., 1986; Harvey et al., 2009). While providing physical movements, these apparati only approximate the true spatial displacement accompanied by appropriate visual information. The visual component can be approximated using Virtual Reality techniques (Aghajan et al., 2015; Hölscher et al., 2005). While improving the nature of visual cues, these methods still require the animal to be fixed, and the visual inputs are necessarily impoverished, both caveats biasing the nature of hippocampal neural computations in ways that are difficult to precisely measure. A method for collecting spatial navigation data in which the direction and speed of the animal can be controlled without restricting the environment or the animal's natural movements is lacking.

Rats are able to learn complex mazes and spatial navigation strategies (de Jong et al., 2011), however, teaching a rat a spatial task usually requires many pre-shaping steps that may or may not influence the manner in which they memorize or recall specific routes in the target task (Skinner, 1953). This difficulty often limits the experimenters, and biases them into choosing tasks that are often simpler than theoretically necessary. Many attempts at imitation or observational learning have been made, in part, to establish whether rats could learn from each other, and perhaps by-pass the pre-shaping phases. Some of the major difficulties in this type of work are making sure that the observer actually pays attention to the demonstrators (non-interacting rats), and that rat interactions do not distract the animals and considerably decrease their learning rate (interacting rats). Improvements in performance can be achieved by cerebellar lesions (Leggio et al., 2003), but the system-wide effect of such lesions on the hippocampus and other structures remains unclear.

One promising technological avenue is to leverage the natural social aptitudes of the rodents using a well-controlled robot. Several research groups have integrated robotics into their investigation of spatial navigation as either a means of interacting with animals or as a way to test a computational model (Cheung et al., 2012; Doya and Uchibe, 2005; Llofriu et al., 2015). Experiments with robots generally focus on how they can influence spatial behavior, social behavior, or learning and memory tasks.

Ho et al. trained rats to follow a manually remote controlled toy car and receive a rewarding intracranial stimulation to the medial forebrain bundle should the animal remain within a specific distance from the car. Simultaneously, they recorded from hippocampal place cells and observed place field remapping and modulation of place cell firing characteristics dependent on the movement and position of the toy car (Ho et al., 2008). These place field modulations, while interesting in and of themselves, make it difficult to study the mechanisms of spatial navigation per se, as place cell firing may be contaminated by social factors and other features associated with the delivery of a reward that is not bound to any physical feature. Additionally, the toy car was controlled manually, and no information was presented regarding the paths taken by the car or how the car's speed fluctuated, if at all.

Other studies have shown that robots have the ability to predictably influence a rat's social behavior by having a rat interact with a rat-like robot displaying friendly, neutral, or stressful activity and observing the rat's resulting behavior post-interaction (Qing et al., 2013). Another study showed that robots may be able to replace one rat within a dyad with minimal effect on the partner when comparing rat-rat interactions to rat-robot interactions in a small environment (del Angel Ortiz et al., 2016). Both studies used an autonomous robot designed to only track and follow the rat at variable speeds, not allowing the robot to emulate random exploration or rat independent navigation. Robots have also been used in experiments exploring predator-prey dynamics in rats, whereby a looming 'predatory robot' caused hippocampal place field remapping depending on the distance between the robot and the rat (Kim et al., 2015). In these experiments, rats were trained to retrieve a food pellet from a narrow high-walled corridor. In some trials, a small robot would surge towards the rat and snap its jaws, eliciting very sudden stressful behavior. These experiments were conducted in relatively spatially constrained environments and were focused on fear processing. In these, and other experiments, the robot is not cooperating with the rat, and presumably could be replaced by other stimuli (spatially moving or not).

In only very few cases have robots been used to teach naïve rats new tasks. For example, rats can be trained to push levers using a lever-carrying robot and a wall-affixed reward distribution apparatus (pellets or water) (Ishii et al., 2006). While the focus was not on spatial navigation in these experiments, the researchers managed to use the robot as a teaching/training tool. Several other recent attempts at designing rat-like robotic devices have also been made successfully, with an emphasis on spatial navigation (Cheung et al., 2012; Wiles et al., 2012). In this work we demonstrate the use of a low cost commercially available robot to aid in behavioral experiments exploring spatial navigation and complex task learning in rodents. Because the robot possesses the ability to be manually or automatically controlled, interact with the rat in a naturalistic manner, allow the rat to move voluntarily, and interact positively with the rat (i.e. no fear conditioning), this method presents the following advantages: (i) The rat's trajectory can be reliably manipulated and replicated, (ii) experimenters can control a rat's absolute speed at any point in the trajectory and (iii) the rat is able to learn from the robot in complex memory tasks in large environments.

2. Methods

2.1. Animals

To demonstrate the feasibility of the framework, we used two 7 months old male Brown Norway rats. The animals were individually housed in Plexiglas cages within a colony room operating on a 24 h reversed light/dark cycle. All experiments were performed during the dark phase of the cycle. The rats were food restricted to within 85% of their ad libitum weight.

2.2. Apparatus

The apparatus used for the experiment was a large open field room (610 × 330 cm), enclosed by 60 cm tall wooden walls. The animal walked on a floor painted with granular water-proof paint to introduce a small amount of roughness and prevent slippage and discomfort to the animals. Walls along the perimeter of the open field, or within the maze (e.g. Fig. 6), were painted solid black on one side, and a mixture of white, black, and grey with various designs on the other in order to provide a cue enriched environment. The

rat's movements were captured by an overhead camera (PointGrey Flea3 at about 60 frames per seconds) mounted on the ceiling in the center of the room. The camera provided inputs to our tracking software ZTracker, written in house in LabVIEW (National Instrument), and freely available from our website. Other USB cameras (e.g. traditional webcams, ~20-30 frames/s) have also been tested successfully. In order to acquire stable tracking data, rats wore a thin strip of Velcro wrapped around their mid-region with reflective tape. A strip of LEDs near the camera provided about 0.5 lux of light during the experiments.

2.3. Sphero

The robot used was a Sphero 2.0 (Sphero, Boulder, CO). The Sphero robot is a small spherical device with a diameter of 7.3 cm and circumference of 23 cm. Sphero weighs approximately 170 g and features a waterproof polycarbonate shell that can be easily washed between experiments. Sphero connects wirelessly via Bluetooth to a Windows 7 workstation and can maintain a stable connection within 100 m of the computer. Additionally, Sphero contains an internal RGB LED with 8 bit intensity resolution for each color. This LED remained OFF during our experiments. Sphero also contains a three-axis accelerometer, a three-axis gyroscope, and an Inertial Measurement Unit to process the data of the previous two components and instantaneously compute yaw, pitch, and roll. The software used to pilot the robot has been developed by the authors and is described below. All instructions are executed and analyzed at about 200 Hz loop-time frequency. Sphero can be purchased with a cart that can be attached and that provides the additional capability of pulling small loads. In most of our experiments the cart carried a small weigh boat in which mash (4:3 food:water) was placed for training purposes. The Sphero-cart assembly has a comparable size and shape to those of a rat. Neither Sphero, nor the cart, have overt moving parts (save for the cart wheels) and the robot produces no human-audible sounds apart from that occurring when the robot moves (wheels on floor).

The battery life of Sphero depends on the type of usage (constant movement or immobility) and was approximately 1–2 h in our experiments. A complete re-charge of the battery takes about 3 h. The maximum input speed command that can be theoretically achieved is 255 cm/s, and during testing in our environment, the highest observed speed achieved without the cart was 230.7 cm/s. With the cart carrying no load, the robot was able to reach a maximum of 177.6 cm/s. Sphero was able to pull about 720 g and still maneuver easily around the open field.

2.4. Tasks

2.4.1. Pre-training

Rats were first exposed to the experimental room for several days, beginning with their home-cage being placed in the environment, and progressing to exploratory/foraging sessions in which the Sphero cart was one of the baited objects. The rats were then habituated to the robot within the same room. The robot and baited cart were placed just outside the home-cage, and then driven slowly around the home-cage. The rat was then placed in the environment and allowed to follow the robot. The entire pre-training process lasted 5–7 days. In addition to the two rats used in this study, we have trained an additional five rats to follow the robot and have found consistent behavior in all animals. Three of these animals were trained in the testing room used in this study (data not shown).

2.4.2. Trajectory manipulations

The robot was first placed on the open field and calibrated for manual joystick control (see software section). It was then connected to the cart and its weigh boat was baited with approximately 0.75–1 g of mash. The rat was then placed in the arena and the experiment began immediately. The robot was piloted manually by the experimenter in order to attract the attention of the rat (simulated darting behavior (Gruene et al., 2015)), eventually resulting in the rat following the robot. Each session lasted about 30 min during which timestamped position coordinates of the rat were recorded with millisecond resolution. When the weigh boat became empty, the robot was kept moving and interacting with the rat for as long as possible until the rat became unresponsive/disinterested, at which time the experimenter re-baited the cart.

2.4.3. Velocity manipulations

As in the previous set of experiments, the robot was initially placed in the room and calibrated before being fitted with the cart and baited with mash. The experiment began as soon as the rat was placed in the environment. The task was to have the rat follow the robot in a figure eight shape that spanned the entire extent of the room, with the intersection point of the figure eight located at the center of the room. Along the two straight path segments of the figure eight (the two linear segments that intersect each other), the experimenter moved the robot at a designated "slow" speed along one of these segments to force the rat to walk behind the robot, and a "fast" speed along the other segment to force the rat to run. Sessions lasted up to 30 min or until the rat remained immobile for several minutes.

2.4.4. Robot-assisted learning

Additional maze walls (approximately 18 cm tall) were used to create a complex maze within the open field. The maze was structured as a non-symmetrical ternary tree with a single start position and two levels (9 branch end-points; see Fig. 6A). A single trial of the task consisted of 2 phases. During the first phase, the rat was guided by the robot. The experimenter pseudo-randomly baited one of the nine reward sites, each located at an end-point, and the robot led the rat from the start position to the correct reward site. The rat was given 10 s to consume the reward (1–1.5 g of mash) before being placed at the start position in an opaque cylinder. The same reward site was then re-baited. The second phase consisted of up to three attempts to find the correct reward location as in the first phase, but without the robot. Finding the reward within three attempts (where visiting any maze branch end-point is considered a single attempt and multiple revisits are considered multiple attempts) resulted in a successful trial. Each day, the rat completed nine consecutive trials in which the reward location was located at each end-point once, but in a different pseudo-random order. The rat was rested for five days before receiving control-testing. These control sessions were run as described previously except that each trial only consisted of the second phase in which the rat had three attempts to find the correct reward location without the robot.

2.5. SpheroControl

The software used to control and acquire data from Sphero was created in house using LabVIEW and is available on the laboratory website for download. Fig. 1 shows the general architecture of the software. The inset shows Sphero (left) with its cart (right). The core of the SpheroControl program (grey box) requires three inputs to calculate the next movement command: tracking coordinates, user-control information (path stored in file, or real-time joystick movements), and feedback from Sphero's internal sensors. Tracking coordinates (X,Y) are received from the tracking software which is paired with the SpheroControl program using Windows' Component Object Model (COM). Control information is divided into two categories: manual and automatic control. Manual control is governed by a joystick (e.g. Microsoft Sidewinder USB Joystick)

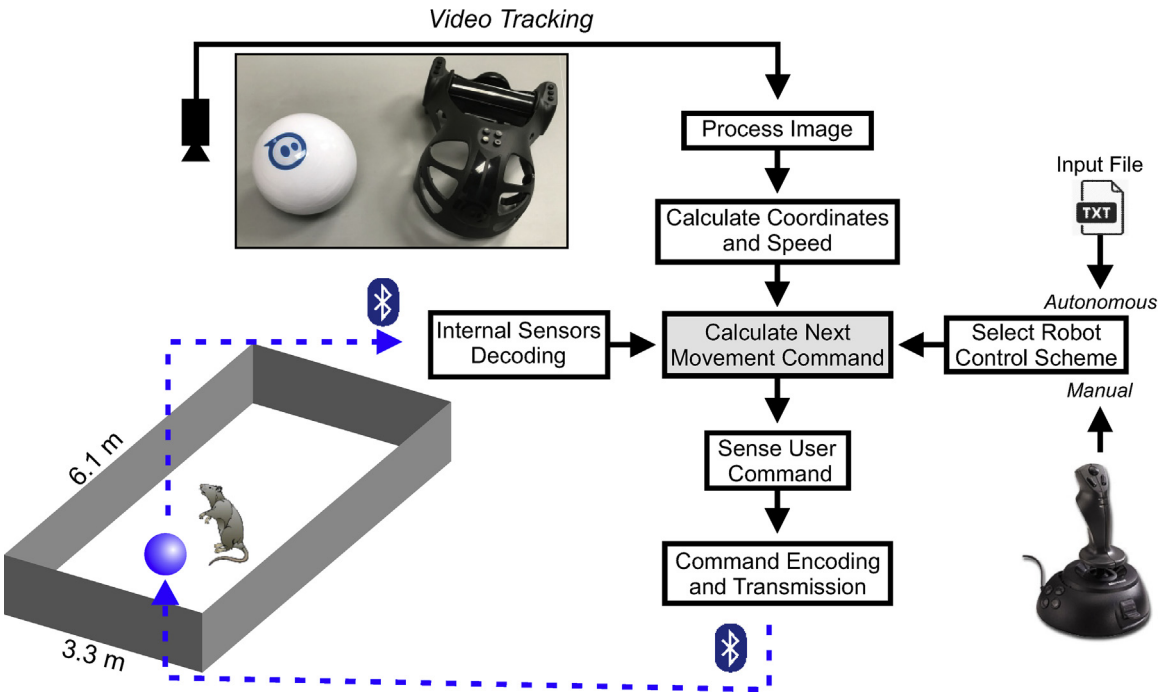

Fig. 1. Behavioral apparatus and Sphero control system. Communication with Sphero is achieved via a standard Bluetooth connection. Maze not to scale. Inset shows Sphero and its cart.

allowing the user to have instantaneous control over the movement and speed of Sphero. Automatic control allows for the loading of an external text file into the program containing target coordinates, the speed (cm/s) at which to approach that coordinate, the duration (seconds) Sphero should stop at each coordinate, and the color Sphero should display on its approach to the current target coordinate. Feedback from Sphero is sent to and received via a Bluetooth connection. Each message packet from Sphero contains information including battery voltage, accelerometer readings, inertial measurement unit data, and speed over ground.

With these three inputs to the program, SpheroControl calculates the corresponding movement command and processes additional options selected by the user. At present, these options include overriding the input file's target speed, pause duration, color, calibration options to adjust the input speed if Sphero is pulling the cart, option to loop the input path ('Patrol mode'), options to save Sphero's speed over ground every timestamp in a new text file, options to save arbitrary user-entered events (millisecond resolution) and options for calibrating the robot's heading.

2.6. Electrophysiology experiment

One of the rats was implanted with a high-density recording device using methods approved by the University of Arizona IACUC and published elsewhere (Valdes et al., 2015). Briefly, the animal was anesthetized using 2–3% isoflurane in oxygen, placed in a stereotaxic frame, and implanted with a Hyperdrive consisting of 14 independently movable tetrodes, 12 of which were aimed at the right dorsal CA1 hippocampal cell body layer (−4.9 mm posterior, 3.8 mm lateral to bregma). All behavioral training paradigms were as described above.

Electrophysiological recordings were made using a wireless Cube 64 device controlled by a Digital Lynx SX system (Neuralynx, Bozeman, MT). Fig. 7A shows an implanted rat with the wireless headstage attached interacting with the Sphero robot. Tetrodes were made of two twisted pairs of 12-μm nichrome wires gold plated to an impedance of 0.5-1 MΩ. Single-unit data was amplified, filtered (600–8000 Hz), and digitized at a rate of 30 kHz. Local field potential was filtered between 0.5–450 Hz, digitized at 2 kHz, and used to detect the presence of sharp wave ripple oscillations, confirming that tetrodes were in the dorsal CA1 cell body layer.

Once single-units were located, the rat was placed in a dimly lit (~0.5 lux) 150 × 150 cm square environment on the floor of the larger room containing unique local cues. This smaller size was chosen to be compatible with traditional environments in which place fields are measured. The rat position was tracked using LEDs mounted on the cube and recorded by the overhead camera as before. The first half of the session consisted of 15 min in which the rat foraged for food pellets, after which the robot with cart affixed and baited with mash, was placed in the environment and an additional 15 min were recorded while the rat followed the robot. The tetrodes were advanced to locate new cells after each session, and were allowed to settle overnight.

Action potentials were sorted offline using a pattern matching procedure with Spike2 (CED, Cambridge UK) and further analyzed using custom Matlab code. Twenty five cells from 11 different sessions were isolated based on firing rate, signal to noise ratio (>4), theta modulation index (>0.5) and refractory period spiking (<1% in the first 3 ms of the autocorrelogram). Tracking and spike data were combined to produce rate maps composed of 11.0 cm^2 bins (Minimum velocity = 10 cm/s). To assess spatial place field remapping, the place fields were computed separately for the foraging and the Sphero-following epochs. The place field maps were vectorized and the Pearson correlations were calculated between the two maps for each session. These correlations were compared to correlations averaged from 10 iterations of shuffled place field maps obtained during different sessions.

3. Results

In order to accurately control the position and speed of a rat with the robot, as well as replicate previous paths and rat trajectories, the behavior of the robot must be consistent and reliable. Integral to the robot's performance is its ability to stop at pre-

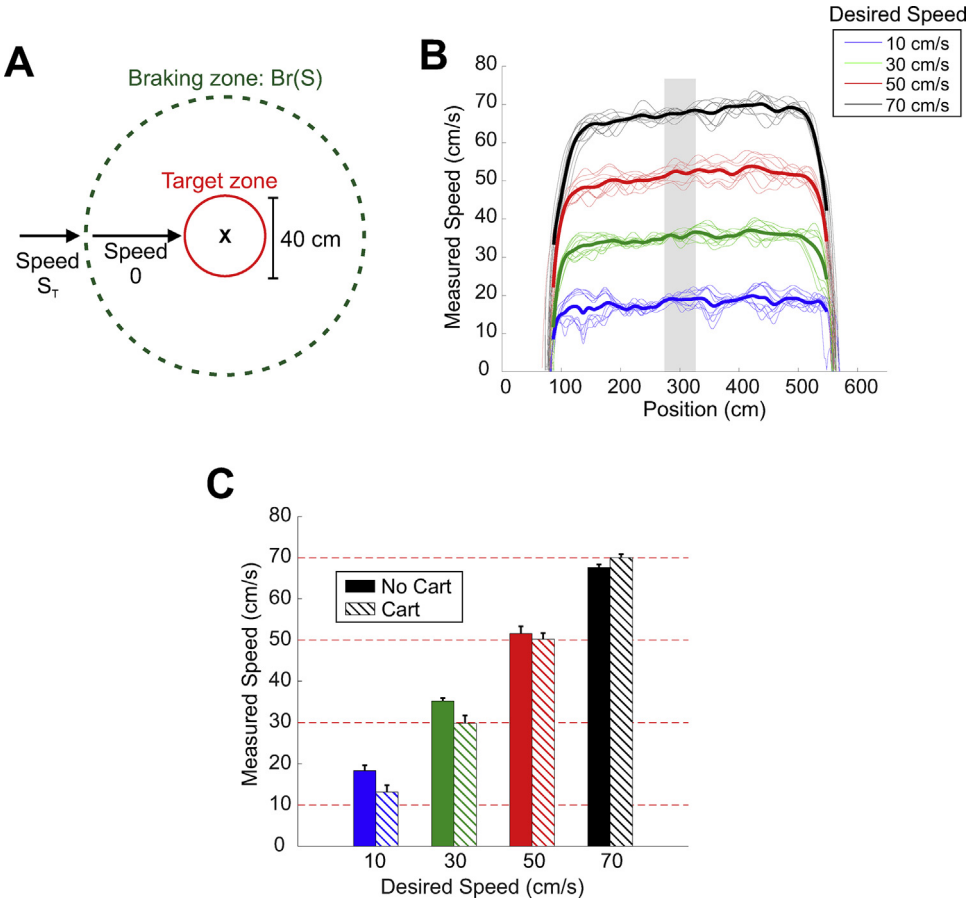

Fig. 2. Reliability of the robot output speed during autonomous navigation. A: Diagram of the robot's braking system. S_T is the current Target Speed. Br(S) is the computed breaking radius. S is the current speed. B: Speed profiles of the robot when commanded to reach a constant speed across the length of the experimentation room. Thicker lines denote the average speed across all trials. C: Average speeds reached at steady state (grey box, in B) for different desired speeds (n = 10 for each desired speed).

cise locations and to exhibit the proper output speed according to its dynamic speed commands. Fig. 2A describes the braking algorithm used by the robot. The *Target zone* is defined as a circular area around the target coordinate (X) where the robot should come to a complete stop and signal that it has reached the target destination. This radius is a user-defined value and cannot be changed while the program is running (here 40 cm). The *Braking zone* (dashed circle) is defined as a larger circular area with radius indicating how far from the target destination the robot must begin stopping procedures in order to come to a complete stop within the *Target zone*. The *Braking radius* Br(S) is dynamically calculated as a function of the robot's current speed (S). Before the robot reaches the *Braking zone*, it is receiving a command speed input (S_T) and exhibits an actual time-dependent speed S. Once it reaches the *Braking zone*, the speed input is set to 0 cm/s. The *Braking Radius* is calculated empirically as an exponential function of actual speed with:

$$Br(S) = 22.37e^{0.02S}\text{cm}$$

Note that the radius is computed at all speeds and will therefore decrease due to a drop in current speed (S). This is advantageous in situations where the robot stops prematurely outside of the target radius but within the braking radius because, when stopped, the braking radius will shrink further to exclude the robot and allow it to resume motion.

For the replication of past trajectories and fine control of a rat's speed, the robot's own speed must be reliable and accurate. Fig. 2B shows the effective speed measured by the tracking software as the robot crossed the long axis of the experimental room (approximately 500 cm used here) 10 times for four representative desired speeds commonly observed in rats (10, 30, 50,and 70 cm/s). The bold lines represent the average speed across the multiple trials for each input speed. On average, the stopping distance for the four target speeds were approximately 4 cm, 15 cm, 15 cm, and 19 cm, respectively, to decelerate from steady speed to a complete stop and approximately 27 cm, 28 cm, 30 cm, and 35 cm, respectively, to reach the desired speed when starting from complete stop (length of the left up-stroke of each average curve). Due to floor friction, the robot had more difficulty achieving lower speeds (10 cm/s), and tended to overshoot the desired speed in order to avoid stalling on irregular and uneven patterns on the ground. Additionally, it can be difficult for the robot to start from rest with slow speeds, and overcome the force required to begin movement. This can be overcome by programmatically setting the departure speed to higher values and quickly decay it to lower desired speed (not shown). Fig. 2B shows that at most speeds, the robot was able to achieve the desired speeds at steady state.

Several factors can influence the robot's speed accuracy, ranging from the load on the cart to the type of flooring. To compensate for this, the software has a tunable parameter (*Friction Factor*) that linearly scales the desired speed, and ensures the ability for different users to run our software according to the specifics of their maze floor. Fig. 2C demonstrates the average speed performance of the robot with or without cart for the four main desired speeds tested in Fig. 2B (i.e. 10 cm/s, 30 cm/s, 50 cm/s, 70 cm/s). In this graph, speeds were measured at the center of the room (grey window in Fig. 2B) and averaged across trials. Without the cart, the robot reached

speeds of 18.29 cm/s, 35.21 cm/s, 51.58 cm/s, 67.62 cm/s, respectively, each sample deviating from the average by less than 2 cm/s. With the cart, the average speeds were 13.14 cm/s, 29.83 cm/s, 50.19 cm/s, 70.04 cm/s, respectively, each sample again deviating from the average by less than 2 cm/s. These experiments were conducted using a *Friction Factor* of zero to simulate the default performance of the robot. With proper tuning of the *Friction Factor*, speeds exactly matching the desired speeds can be achieved within similarly low deviation from the mean (not shown). The simple linear breaking model used here allowed for fast parameter adjustments and flexibility. Future work will explore the use of other, more refined models and speed control strategies including those that rely on a proportional-integral-derivative (PID) controller.

One major benefit of the SpheroControl program is its accuracy in autonomous navigation mode and its ability to replicate previously recorded paths. These paths can be 1) from previous trials/sessions, 2) from idealized paths computed off line according to explicit equations or a computational model or 3) from experiments involving the tracking of an actual rat. Such replicability is of paramount importance for scientific investigations. Fig. 3A compares the trajectories of separate instances of the completion of a task in a 1.5 m diameter open field used in previous work (Jones et al., 2012). Along the border of the open field are eight evenly spaced feeders of which only one will release a drop of sugar water reward at any given time. Each feeder is fitted with a blinking LED indicating the availability of the reward. Once the reward has been received, a new feeder is pseudo-randomly cued. A session stops after the animal has consumed approximately 200 rewards. The leftmost graph shows the trajectory of a trained rat performing a single session of this experiment. The center graph shows the trajectory of the robot when only given the coordinates of the reward locations in the same sequence as the rat. In this scenario, the robot should ideally navigate between each feeder in quasi-straight lines. The rightmost graph shows the trajectory observed when Sphero was given the coordinates obtained from the rat's track data in the leftmost graph. For comparison, 4 corresponding paths are highlighted in the 3 conditions.

Fig. 3B quantifies the path variability from Fig. 3A. Path variability is defined as the average deviation (cm) from the optimal straight-line path drawn between the start and end points of a single path segment (the traversal between two reward locations). The rat navigated with an average deviation from the straight-line path of 8.52 ± 7.24 cm (n = 225). The robot, after being given the coordinates of the target reward locations achieved an average deviation of 2.36 ± 2.90 cm (n = 189). When given the coordinates from the rat trajectory, the robot exhibited an average deviation from straight-line segments of 4.68 ± 4.12 cm (n = 214). These results show that the robotic framework can effectively allow for the control of the robot over multiple and repeated path segments, whether these segments are specified as targets (3A, center) or whether they are specified continuously to replicate a given rodent behavior (3A, right).

3.1. Trajectory manipulations

It is notoriously difficult to train a rat to travel along the same exact trajectory more than once in an open field environment. We next assessed whether a rat can be taught to follow our robot in a consistent and reliable manner. This was achieved by baiting the cart (Fig. 4A, see methods). Note that the animal wore a small reflective belt for tracking purposes.

With the use of the robot, the rat can be led to create and recreate different patterns within a bare open field (no interior walls, objects, or reward locations). In Fig. 4B, the rat followed the robot to create a four-leaf clover navigation design. Such a pattern shows the ability of the system to manipulate the rat trajectory and traverse the same location (intersection point) using several, well controlled, approach angles. Should a place field be identified in an open field experiment, our robot can be used to control the rat's entry into the place field from many different directions and observe how direction of movement influences the place cell firing activity.

Fig. 4C demonstrates the robot's ability to lead the rat along several parallel straight-line paths, simulating a hairpin maze without the use of any walls. The rat was able to traverse the maze without walking through the imaginary boundaries that are known to contribute to field segmentation and remapping in the walled version of the task.

In addition to controlling the angle of entry in a spatial zone and simulating standard research mazes, the robot is able to lead the rat to travel along a variety of different movement patterns. In Fig. 4D, as a means of demonstration, the robot leads the rat to spell out the letters "CENL". The 'C' demonstrates the ability to create large swooping, circular paths. The 'E' shows the ability to create very straight paths as well as perform right angle turns (top and bottom bars of the 'E') as well as double backing/180° turns (middle bar of the 'E'). The 'N' demonstrates straight paths as well as very tight angle turns (15° and 16° for the turn inner angles of the 'N'). The 'L' further shows the ability to travel a T-maze-like path.

3.2. Velocity manipulations

Of equal importance to the ability to directly manipulate a rat's trajectory is the ability to control the speed of the animal. The speed of the rat can be controlled by training the animals to follow the robot, whatever its speed. To illustrate this manipulation, the robot led the rat in a figure-eight pattern that included two straight-line segments (Fig. 5A, red and green). The experimenter moved the robot at slow speed on one segment (approximately 20 cm/s, green) to elicit walking behavior, and at fast speed (approximately 55 cm/s, red) along the other segment to elicit running behavior.

Fig. 5B shows the speed profile of the rat for the two linear segments of the figure-eight, as a function of the rat's horizontal position in the environment. The thicker lines denote the average speed across trials. The grey interval in the center of the graph denotes the location of the intersection point within the figure-eight shape.

The quantification of the results shown in panel B are shown in Fig. 5C, displaying the average running and walking speeds across all trials (running: n = 34, walking: n = 25) as well as their standard deviation from the mean at the intersection point of the figure-eight. In running trials, the rat traveled at an average speed of 55.83 ± 9.30 cm/s. Walking trials yielded an average traveling speed of 19.60 ± 5.51 cm/s. These two datasets were significantly different. Based on these results, we show that the robot is able to reliably control the rat's speed.

3.3. Robot-mediated learning

We next tested whether the robot would be able to improve the rat's performance in a memory task in a large environment. We used a branching maze in the shape of a two level ternary tree: A maze with a single start position and two levels of 3-decisions points, for a total of nine branch end-points (Fig. 6A).

We measured the ability for the robot to improve the rat's performance in a complex memory task by assessing the number of successful trials performed by the rat with or without the aid of the robot (see methods). Over the course of nine sessions, the rat showed an increase in the number of successful trials in which it found the correct reward location with the aid of the robot (Sphero, Fig. 6B). In this experiment, the rat could not learn without the robot's assistance (Control, Fig. 6B). In these control trials, the rat's

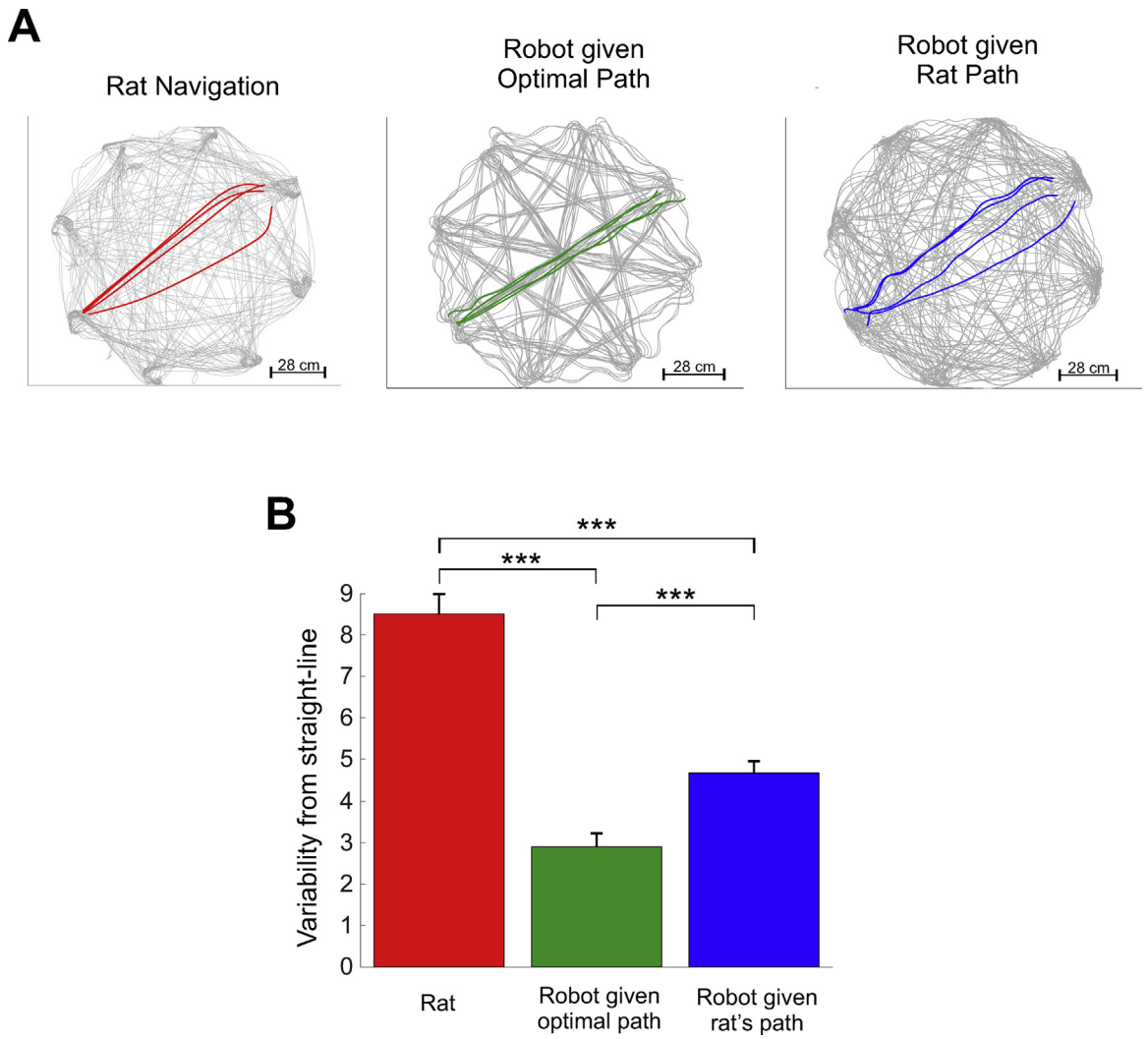

Fig. 3. The robot is precise enough to replicate rat-like trajectories. A: Tracking data of a rat (left), the robot given an optimal straight-line trajectory (middle), and the robot given the rat's track data as a trajectory input (right). Four representative path segments are highlighted. B: Average variability from the straight-line optimal path from the track data in the task shown in A.

performance was commensurate with the predicted performance operating at chance, demonstrating that the rat was unable to use any other strategy to solve the maze (i.e. smelling the reward or hearing the experimenter place the reward).

In addition to counting the number of successful trials performed by the rat, we examined how often the rat made an error in a given session, averaged across all trials. Because the rat was given three opportunities to find the correct reward location, the average errors per session ranged between 0 and 3. Fig. 6C shows the number of errors over the course of the nine sessions for both robot aided (Sphero) and non-aided (Control) sessions. Similar to the previous results, control trials demonstrated little to no change across sessions whereas robot-aided trials yielded a decrease in errors over time. The last three sessions showed a significant difference in the number of errors between the control and the robot-aided sessions.

Another indicator of the rat's performance can be seen in the number of times a successful trial was achieved on the first of three attempts, for any given reward location. Fig. 6D shows the total number of correct first attempts for all sessions in both aided and non-aided sessions. Again, in the non-aided (control) trials, the rat performed at or near chance levels (dashed line). However, in the robot-aided sessions, overtime the rat's number of successful first attempts within a session increased to levels well above chance.

3.4. Robot influence on place fields

Previous methods of controlling a rat's spatial navigation using a moving object have been shown to alter the characteristics of a place cell firing field (Kim et al., 2015; Terrazas et al., 2005). We next tested whether the following behavior of the animal in the presence of Sphero had a significant influence on the spatial characteristics of hippocampal place fields. We recorded place cells from the dorsal CA1 area of the hippocampus during 25 sessions. Each session consisted of a 15 min classic foraging session (no robot) immediately followed by a 15 min session in which the rat was encouraged to follow Sphero, as before (see methods). Fig. 7B displays the place fields from two different place cells (different tetrodes) recorded simultaneously during the foraging phase (left) and during the subsequent robot phase (right). As can be seen in these representative examples, there was no remapping because of the robot-following behavior.

Foraging and robot-following place-fields were compared by conducting a bin-wise correlation between two place fields, where values close to 1 indicate high spatial correlation and minimal remapping, and values close to 0 indicate complete remapping. These results are shown in Fig. 7C averaged across the 25 sessions. When the place field of the foraging phase was compared

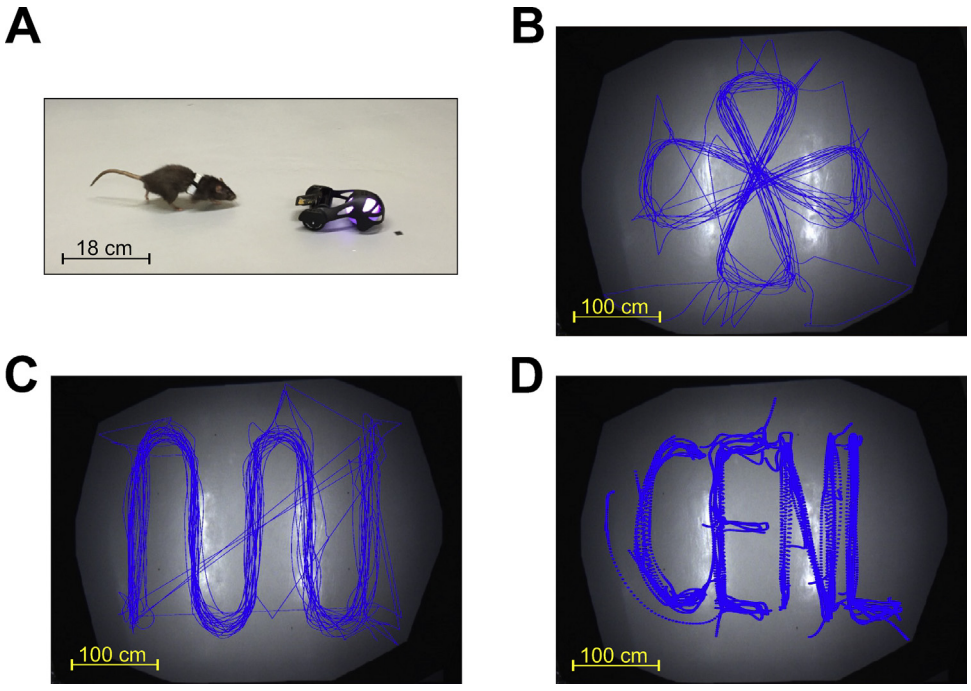

Fig. 4. Tracking data from the rat during rat-robot interaction sessions demonstrating control over unique path shapes. A: Still image from an interaction session showing a rat following Sphero and its cart. B: Four-leaf clover shape showing the control of travel angle. C: Simulated hairpin maze with no walls present. D: Arbitrary path to spell "CENL" displaying control over several types of trajectories containing different turn angles (approximately 90° and 180° in 'E', 15° and 16° in 'N').

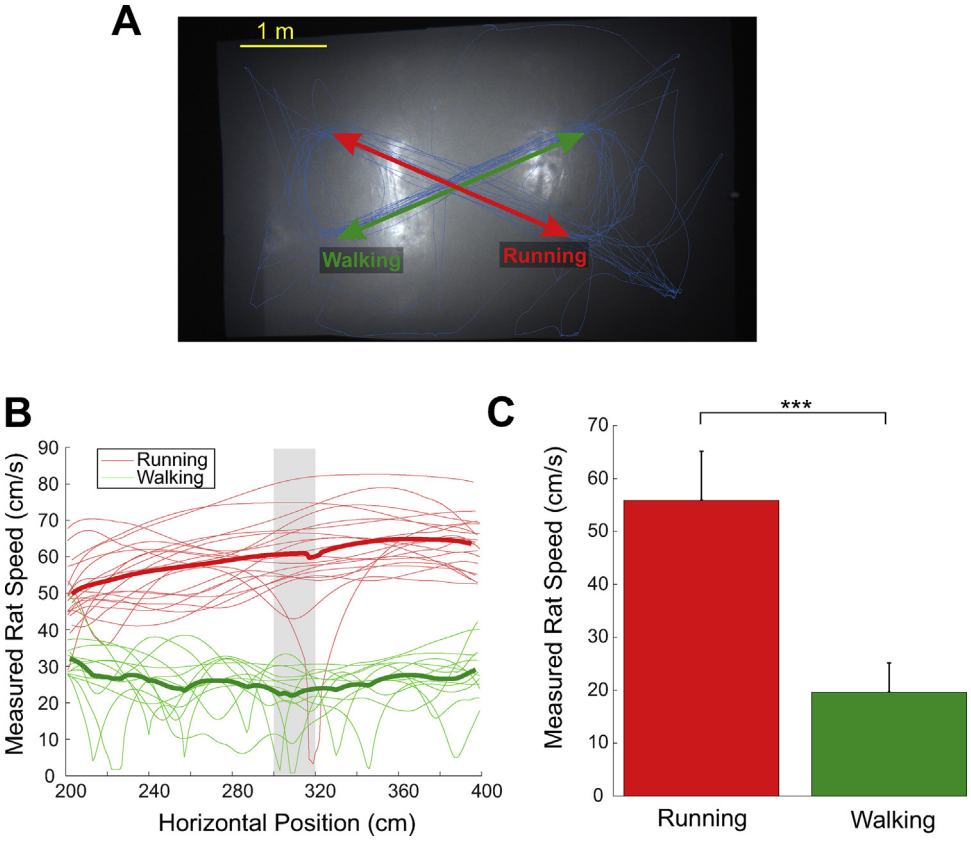

Fig. 5. The rat's speed can consistently be manipulated by the speed of the robot. A: Figure eight pattern used to guide the rat through the same central location from different angles at different speeds (running and walking). B: Speed profile of the rat along the two straight paths of the figure eight. Thick lines show the average speed across all trials. The shaded region indicates the center point of the figure eight. C: Rat's average speed across multiple trials (Running n = 34, Walking n = 25) in the figure eight (One-way ANOVA, $F[1,56]$, $P < 0.0001$).

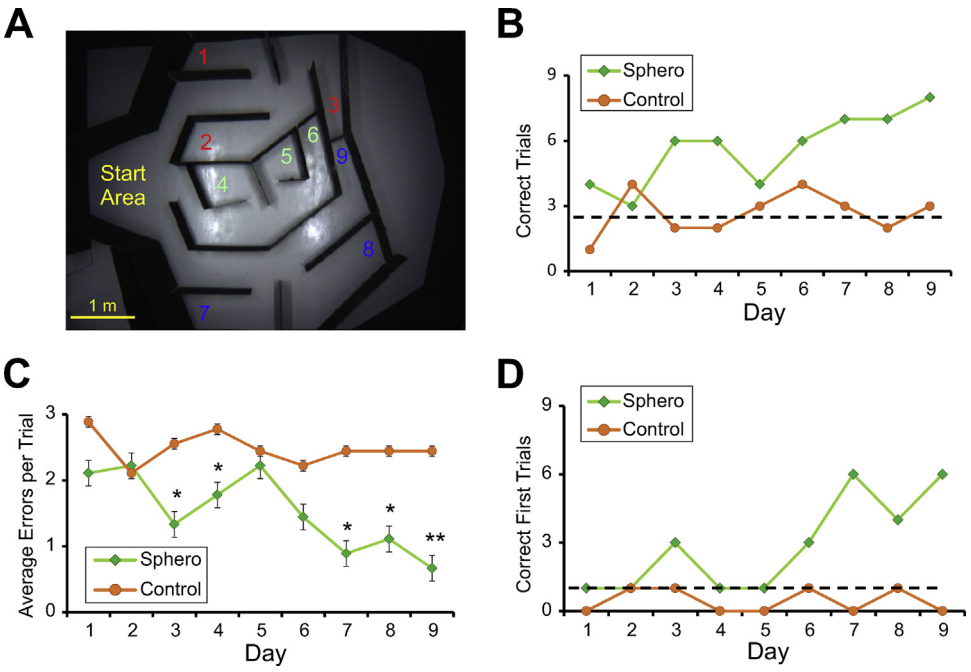

Fig. 6. Example of a spatial learning task involving rat-robot interactions. In the robot condition (Sphero), the robot showed the animal the correct path on one trial, and the animal was given up to 3 subsequent trials to find the reward alone. A: Overhead view of the maze showing the nine possible reward locations. Numbers of the same color represent reward locations found in the same major branch. B: Number of trials the rat successfully found the reward within three attempts across nine sessions. C: Average number of errors per trial across nine sessions. D: Number of times the rat visited the correct reward location on first attempt across nine sessions.

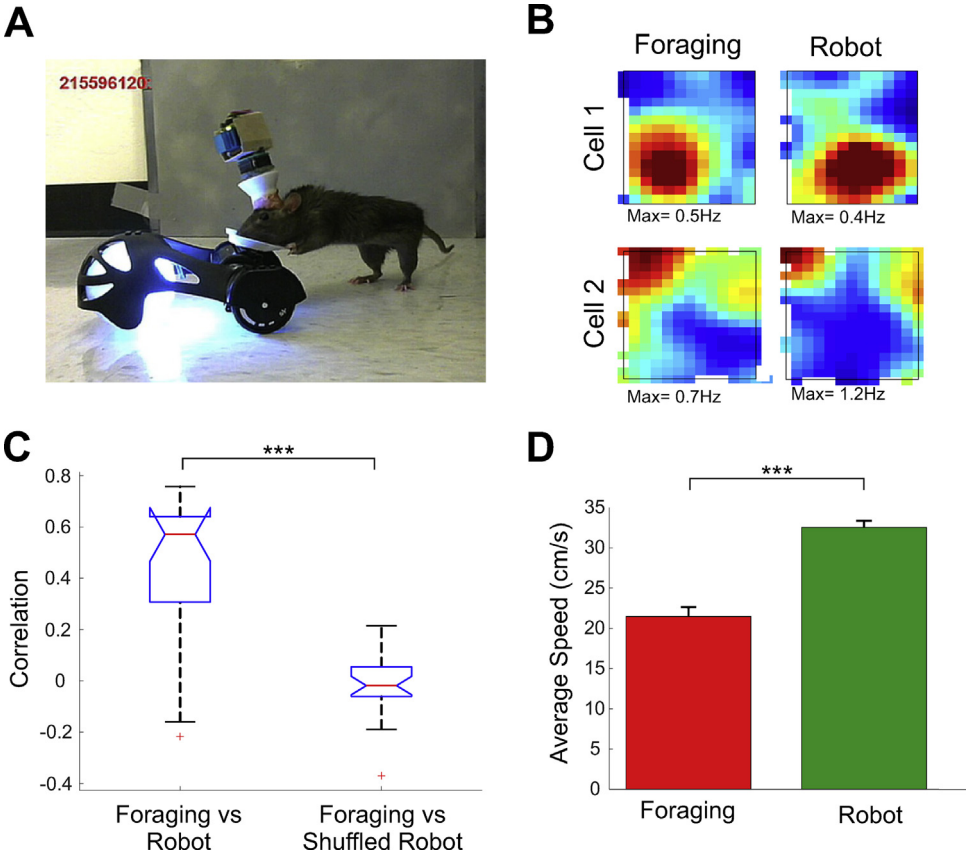

Fig. 7. Analysis of Place fields with and without the influence of the robot. A: Rat with implanted hyperdrive and wireless headstage interacting with the robot. B: Two examples of place fields recorded simultaneously with (right) and without (left) robot interactions. C: Distribution of the spatial correlations between Foraging and Robot trials of the same sessions compared to the correlations of shuffled sessions (n = 10 shuffles, One-way ANOVA, $P < 0.0001$). D: Comparison of the average rat moving speed in Foraging trials and Robot trials (One-way ANOVA, $P < 0.0001$).

to its corresponding robot phase of the same session, the median correlation was 0.5708, with a mean correlation of 0.4432. One outlier skewed the distribution slightly. Within the shuffled sessions, the median correlation was −0.0184 and the mean was −0.0060, showing that the controlled shuffled data contained no correlation, as expected. The two sets were significantly different from each other ($P < 0.001$, one-way ANOVA). Across the population of cells recorded, the maximum firing rate of place cells were not significantly different between the foraging ($1.19\,Hz \pm 0.21$) and Sphero ($1.28\,Hz \pm 0.28$) sessions.

During the foraging phase, the rat traveled at 21.48 ± 1.13 cm/s, while it traveled at 32.55 ± 0.80 cm/s across all 25 sessions in the Sphero following phase, shown in Fig. 7D. These results demonstrate that the rat was able to move faster with the aid of the robot than when by itself, even in a foraging task.

4. Discussion

We proposed a new paradigm for rodent spatial navigation studies. Using a small and fully controllable robot, we showed that we were able to manipulate the precise trajectory and speed of the animal. We also showed that the robot could be used to teach the rat the correct path in a complex maze with 9 possible reward sites using a single teaching trial. Finally, we showed that the use of the robot in these conditions did not produce significant place field remapping, allowing for the design of new robot-assisted experimental protocols aimed at understanding the mechanisms of complex spatial navigation (Harland et al., 2017).

In the past, in order to motivate a rat to follow a somewhat complex trajectory (e.g. sharp turns, double backing, multiple repetitions, etc.) experiments relied on restrictive environmental factors. These included using narrow-walled corridors, restraining the rat to a researcher controlled device, or restraining the rat to a single position using treadmill like movement to simulate navigation in a real or virtual environment. The use of a robot offers a non-stressful alternative to these restrictive paradigms and in addition allows for the conduct of experiments in large and complex spaces. For example, we were able to control the rat's path to create a four leaf clover shape and simulate a wide corridor hairpin maze without the use of any interior walls. Key to these experiments is that the rat traversed these paths voluntarily, under its own locomotion, in order to collect a reward. Additionally, the rat was given only a positive motivator to achieve this performance, there was no negative reinforcement or fear conditioning involved. Using the robot to guide the navigation of a rat during electrophysiological recordings could have several advantages. Firstly, we could motivate the rat to achieve a greater average speed compared to un-directed foraging, facilitating greater coverage over time in a large environment. Moreover, this method could be used to provide consistent coverage of all quadrants of a room throughout a recording session, which could be particularly useful in studying the dynamics of spatially tuned cells. Lastly, once a spatially tuned cell is located we could guide the rat to move through the cell's field(s) from multiple well-controlled directions and speeds.

With the ability to manipulate the rat's trajectories comes the natural extension of controlling the rat's speed. Our results show the ability to manipulate the speed of the animal from walking to running (or any other intermediate speeds) by precisely controlling the velocity of the robot. The ability to control a rat's speed, whether in a structured maze or an open environment is important because of the known role of velocity in influencing the neural encoding of movement (Ahmed and Mehta, 2012; Huxter et al., 2003; McNaughton et al., 1983; Sheremet et al., 2016; Zheng et al., 2015). Short of measuring speed post-hoc, studies aimed at manipulating the speed of a rat relied on binding the rat to a treadmill or ball and navigating through a well-controlled virtual environment. In our study, the rat moves of its own volition in a real environment which elicits a more realistic and natural behavior. This self-motion is an important aspect of rat spatial navigation, which is key to yielding realistic place cell activity (Lu and Bilkey, 2010). Because the user can control the rat speed within 2 or 3 cm/s, this system will allow for future experiments aimed at understanding the influence of movement speed on neural coding in the hippocampus and other structures. For example, it may be interesting to further explore the relationship between locomotion and hippocampal theta oscillations (Long et al., 2015) or re-examine the functionality of medial entorhinal speed cells (Kropff et al., 2015) using our robotic framework.

Many classical experiments aimed at elucidating the neural mechanisms of spatial navigation have focused on small and relatively simple environments. The limitation is at least in part due to technical constraints regarding the data acquisition method (tethered system) and the training paradigms (experimenter-dependent pre-shaping). We were able to use our system in very large environments and showed its compatibility with a high-density wireless system. We also showed that the robot could be effectively used to teach the rat a complex spatial memory task. Our results suggest that the use of the robot induced an increase in performance in finding rewards in an environment too large and too complex for the rat to learn by itself within the time frame of an experimental session. These results show that the robot could not only be used to manipulate a rat's actual spatial navigation, but could also potentially be used to 'remove' the experimenter from the room and be used as an ethologically realistic aid to teach rats a complex task with minimal experimenter intervention. Indeed, using this robotic framework alongside automated long-term recording techniques, would allow for paradigms in which the rat could live with minimal human interactions whilst only interacting/doing tasks with the robot. In the nine-goal maze task, the robot leads the rat to a reward location, a procedure that could be adapted to other kinds of spatial tasks or during pre-training phases to increase the efficiency of behavioral shaping. With a proper wall-avoidance software, the robot can be used in spatial tasks featuring narrow maze arms such as radial-arm and T-mazes. Furthermore, a specialized cover enables Sphero to operate on water and could be used to guide rats to the platform location in the water maze.

While our robotic framework offers many benefits for future behavioral experimentation, it has some limitations. Because the robot is able to travel using a wide array of speeds, it is best suited for use in a large environment. When used in a small environment, the robot is likely to hit the environment boundaries when traveling above a certain speed threshold. As with any robot, Sphero is limited by its battery life (about 1 h). To the extent that the robot is low cost, this can be easily addressed by using three Spheros and swapping and recharging them when necessary, yielding virtually endless use. A second limitation is the necessity of an overhead tracking camera in autonomous navigation mode. Sphero corrects its position using feedback from the tracking software, so all areas of the maze have to be visible to the camera. An alternative would be to fit a camera on the cart and process local visual information. We note that this feedback is akin to visual information from the lateral entorhinal cortex, while internal sensors are akin to self-motion information from the medial entorhinal cortex. In principle therefore, Sphero could be used as an autonomous entity to test various entorhinal-hippocampal models of spatial navigation, possibly extending to planning (prefrontal cortices) and reward (Striatum or ventral tegmental area) systems (Llofriu et al., 2015).

We demonstrated that robot-guided navigation did not result in significant place-cell remapping after a robot-free, classical foraging session in the same environment. The ability of the rat to learn the nine-goal maze demonstrates that the rat is aware of the

route taken during the robot-guided portion of the trial. In these conditions, the rat's behavior is therefore akin to *bona fide* spatial navigation. Interestingly, chasing the moving robot constitutes a kind of dynamical goal-directed behavior in which the reward is constantly moving. Such behavior may be fundamentally different from that of foraging or fixed goal path planning, and may recruit brain areas in ways that have not been shown before. The neural correlates of these different types of navigation needs to be further investigated and contrasted, and the nature of the contribution of the hippocampus to each of these navigation types needs to be clarified.

In summary, the current study demonstrates a novel approach to controlling a rat's movement and speed during behavioral and electrophysiological experiments using a robotic framework. Our hope is that this approach may provide a new way of examining the functional properties of spatially tuned neurons in the brain as well as facilitate the creation of novel behavioral and electrophysiological paradigms.

Significance statement

We propose a novel robotic framework aimed at rodent spatial navigation experiments. We show that the robot can precisely follow predetermined or user-controlled trajectories, that rats can be trained to follow the robot on those same trajectories and that the robot is able to teach the rat in complex and large environments. We also show that CA1 place fields do not remap because of the robot. This framework could potentially be used to test novel hypotheses in ethologically realistic spatial environments and derive new training and task paradigms that may give further insight into the neural substrate of spatial navigation.

Funding

ONR MURI: N000141310672, N000141612829, N000141512838.

Conflict of interests

None.

Acknowledgments

The authors would like to acknowledge Blaine Harper, Emma Armstrong, Michael Ragone and Dr. Tatiana Pelc for their help.

References

Aghajan, Z.M., Acharya, L., Moore, J.J., Cushman, J.D., Vuong, C., Mehta, M.R., 2015. Impaired spatial selectivity and intact phase precession in two-dimensional virtual reality. Nat. Neurosci. 18, 121–128.

Ahmed, O.J., Mehta, M.R., 2012. Running speed alters the frequency of hippocampal gamma oscillations. J. Neurosci. 32, 7373–7383.

Cheung, A., Ball, D., Milford, M., Wyeth, G., Wiles, J., 2012. Maintaining a cognitive map in darkness: the need to fuse boundary knowledge with path integration. PLoS Comput. Biol. 8, e1002651.

del Angel Ortiz, R., Contreras, C.M., Gutiérrez-Garcia, A.G., González, F.M.M., 2016. Social interaction test between a rat and a robot: a pilot study. Int. J. Adv. Rob. Syst. 13, 1–10.

de Jong, L.W., Gereke, B., Martin, G.M., Fellous, J.M., 2011. The traveling salesrat: insights into the dynamics of efficient spatial navigation in the rodent. J. Neural Eng. 8, 065010.

Derdikman, D., Whitlock, J.R., Tsao, A., Fyhn, M., Hafting, T., Moser, M.-B., Moser, E.I., 2009. Fragmentation of grid cell maps in a multicompartment environment. Nat. Neurosci. 12, 1325–1332.

Doya, K., Uchibe, E., 2005. The Cyber Rodent Project: Exploration of Adaptive Mechanisms for Self-Preservation and Self-Reproduction. Adapt. Behav. 13, 149–160.

Foster, T., Castro, C.A., McNaughton, B.L., 1989. Spatial selectivity of rat hippocampal neurons: dependence on preparedness for movement. Cell 6, 4.

Fox, S.E., Wolfson, S., Ranck, J.B., 1986. Hippocampal theta rhythm and the firing of neurons in walking and urethane anesthetized rats. Exp. Brain Res. 62, 495–508.

Gruene, T.M., Flick, K., Stefano, A., Shea, S.D., Shansky, R.M., 2015. Sexually divergent expression of active and passive conditioned fear responses in rats. eLife 4, e11352.

Harland B, Contreras M, Fellous J (2017) A Role for the Longitudinal Axis of the Hippocampus in Multiscale Representations of Large and Complex Spatial Environments and Mnemonic Hierarchies. In: Hippocampus (Stuchlik A, ed).

Hölscher, C., Schnee, A., Dahmen, H., Setia, L., Mallot, H.A., 2005. Rats are able to navigate in virtual environments. J. Exp. Biol. 208, 561–569.

Harvey, C.D., Collman, F., Dombeck, D.A., Tank, D.W., 2009. Intracellular dynamics of hippocampal place cells during virtual navigation. Nature 461, 941–946.

Ho, S.A., Hori, E., Kobayashi, T., Umeno, K., Tran, A.H., Ono, T., Nishijo, H., 2008. Hippocampal place cell activity during chasing of a moving object associated with reward in rats. Neuroscience 157, 254–270.

Huxter, J., Burgess, N., O'keefe, J., 2003. Independent rate and temporal coding in hippocampal pyramidal cells. Nature 425, 828–832.

Ishii, H., Ogura, M., Kurisu, S., Komura, A., Takanishi, A., Iida, N., Kimura, H., 2006. Experimental study on task teaching to real rats through interaction with a robotic rat. In: Nolfi, S., Baldassarre, G., Calabretta, R., Hallam, J.C.T., Marocco, D., Meyer, J.-A., Miglino, O., Parisi, D. (Eds.), From Animals to Animats 9: 9th International Conference on Simulation of Adaptive Behavior, SAB 2006, Rome, Italy. September 25–29, 2006. Proceedings. Springer Berlin Heidelberg: Berlin, Heidelberg, pp. 643–654.

Jones, B., Bukoski, E., Nadel, L., Fellous, J.-M., 2012. Remaking memories: reconsolidation updates positively motivated spatial memory in rats. Learn. Mem. 19, 91–98.

Kim, E.J., Park, M., Kong, M.-S., Park, S.G., Cho, J., Kim, J.J., 2015. Alterations of hippocampal place cells in foraging rats facing a 'predatory' threat. Curr. Biol. 25, 1362–1367.

Kropff, E., Carmichael, J.E., Moser, M.B., Moser, E.I., 2015. Speed cells in the medial entorhinal cortex. Nature 523, 419–424.

Leggio, M.G., Graziano, A., Mandolesi, L., Molinari, M., Neri, P., Petrosini, L., 2003. A new paradigm to analyze observational learning in rats. Brain Res. Brain Res. Protoc. 12, 83–90.

Llofriu, M., Tejera, G., Contreras, M., Pelc, T., Fellous, J.M., Weitzenfeld, A., 2015. Goal-oriented robot navigation learning using a multi-scale space representation. Neural Netw. 72, 62–74.

Long, L.L., Bunce, J.G., Chrobak, J.J., 2015. Theta variation and spatiotemporal scaling along the septotemporal axis of the hippocampus. Front. Syst. Neurosci. 9, 37.

Lu, X., Bilkey, D.K., 2010. The velocity-related firing property of hippocampal place cells is dependent on self-movement. Hippocampus 20, 573–583.

McNaughton, B., Barnes, C.A., O'keefe, J., 1983. The contributions of position, direction, and velocity to single unit activity in the hippocampus of freely-moving rats. Exp. Brain Res. 52, 41–49.

Navratilova, Z., Hoang, L.T., Schwindel, C.D., Tatsuno, M., McNaughton, B.L., 2012. Experience-dependent firing rate remapping generates directional selectivity in hippocampal place cells. Front. Neural Circuits 6, 6.

Qing, S., Hiroyuki, I., Shinichi, K., Atsuo, T., Satoshi, O., Naritoshi, I., Hiroshi, K., Shigenobu, S., 2013. Modulation of rat behaviour by using a rat-like robot. Bioinspiration Biomimetics 8, 046002.

Sheremet, A., Burke, S.N., Maurer, A.P., 2016. Movement enhances the nonlinearity of hippocampal theta. J. Neurosci. 36, 4218–4230.

Skinner, B.F., 1953. Science and Human Behavior. Macmillan, New York.

Terrazas, A., Krause, M., Lipa, P., Gothard, K.M., Barnes, C.A., McNaughton, B.L., 2005. Self-motion and the hippocampal spatial metric. J. Neurosci. 25, 8085–8096.

Valdes, J.L., McNaughton, B.L., Fellous, J.M., 2015. Offline reactivation of experience-dependent neuronal firing patterns in the rat ventral tegmental area. J. Neurophysiol. 114, 1183–1195.

Whitlock, J.R., Derdikman, D., 2012. Head direction maps remain stable despite grid map fragmentation. Front. Neural Circuits 6, 9.

Wiles, J., Heath, S., Ball, D., Quinn, L., Chiba, A., 2012. Rat meets iRat. 2012 IEEE International Conference on Development and Learning and Epigenetic Robotics (ICDL), 1–2.

Zheng, C., Bieri, K.W., Trettel, S.G., Colgin, L.L., 2015. The relationship between gamma frequency and running speed differs for slow and fast gamma rhythms in freely behaving rats. Hippocampus 25, 924–938.